Light- and humidity-driven actuators with programmable complex shape-deformations

Luzhuo Chen[a,b,c,*], Mingcen Weng[a,b,c], Feng Huang[a,b,c], Wei Zhang[a,b,c]

[a] Fujian Provincial Key Laboratory of Quantum Manipulation and New Energy Materials, College of Physics and Energy, Fujian Normal University, Fuzhou 350117, China
[b] Fujian Provincial Collaborative Innovation Center for Optoelectronic Semiconductors and Efficient Devices, Xiamen 361005, China
[c] Fujian Provincial Engineering Technology Research Center of Solar Energy Conversion and Energy Storage, Fuzhou 350117, China

ABSTRACT

Programmable complex shape-deformation, multi-responsive property and convenient fabrication are all crucial for the development of actuators. However, a simultaneous realization of all these advantages has not been reported. Here, we report a new type of light- and humidity-driven actuator with programmable complex shape-deformations. The fabrication employs a laser printing technology. The light-driven actuation is based on a dual-mode actuation mechanism which utilizes the water adsorption/desorption properties. When irradiated by near infrared light, the actuator shows a large bending actuation with a curvature up to $2.1\,\mathrm{cm}^{-1}$. More importantly, programmable complex shape-deformations can be realized by printing patterns with different/gradient grayscale distributions on the actuators. The bending rates and amplitudes of actuators can be programmed and controlled. Complex 3D shapes, such as an anomalous tube and a helical cylinder, are obtained. In addition, the actuator can also perform a curvature of $1.3\,\mathrm{cm}^{-1}$ when driven by humidity. Finally, a series of smart biomimetic devices with programmable complex shape-deformations are demonstrated, including a self-adjustment iris responding to incident light, a biomimetic hand demonstrating a complex "OK" gesture, and a lotus with folding petals of different bending rates. This new-type actuator will have great potential in robotics and biomimetic applications.

1. Introduction

Smart actuating materials perform shape-deformations when triggered by an external stimulus, such as light [1–6], electricity [7–10], humidity [11–15], heat [16–18], magnetism [19], solvents [20,21] and pH [22]. They have important applications in the fields of artificial muscles, bionic iris, soft robotics, optical switches and so on [23–25]. Among them, bilayer actuators based on carbon nanotubes or graphene sheets are widely reported, in which the shape-deformations are due to asymmetric deformations of two layers in the actuators [4,6,8,12,13,26–28]. The deformation of these actuators is usually limited to simple elongation [9] and bending [6,8,12,26–28]. Only a few of them can perform helical deformations [4,13]. However, more complex shape-deformations, which are important for further applications, are rarely reported. The reason is that the key point of realizing programmable complex shape-deformations is to distinctively and locally control the deformation of specific parts of the actuators, which is still a great challenge for the reported actuators. Recently, the fabrications of actuators with programmable complex shape-deformation by

printing technologies have been developed in hydrogels and shape memory materials [29–31]. There is still plenty of room for the improvement of fabricating actuators with programmable complex shape-deformation through a more convenient printing method. In addition, most of the actuators are driven by a single stimulus, which limits their application field. There were only several studies on multi-responsive actuators [32–34]. They can be used under various environment and broaden the application fields of actuators. Nevertheless, the development of multi-responsive actuators with a fast fabrication method and programmable complex shape-deformations is still challenging and requires further research.

Here, we report light- and humidity-driven actuators with programmable complex shape-deformations. The key fabrication process is printing black toner on the paper by using a laser printer. The actuator has a bilayer structure consisting of toner-coated paper (TCP) and biaxially oriented polypropylene (BOPP). Compared with previous actuators fabricated through complicated synthetic steps, our fabrication method is fast and solution-free. Furthermore, with the aid of laser printing technology, we can fabricate precisely-patterned actuators in

an inexpensive way. The TCP/BOPP actuator can perform a maximum bending curvature of $2.1\,cm^{-1}$ when driven by near infrared (NIR) light. More importantly, programmable complex shape-deformations can be realized by introducing patterns with different/gradient grayscale distributions on the TCP/BOPP actuators. With this advantage, the bending rates and amplitudes of actuators can be programmed and controlled by using our route. We also demonstrate programmable complex 3D shapes, such as an anomalous tube and a helical cylinder, which have not been reported in previous carbon-based actuators. On the other hand, the TCP/BOPP actuator also shows a maximum bending curvature of $1.3\,cm^{-1}$ when driven by humidity. Finally, a series of biomimetic devices including a self-adjustment iris, a hand demonstrating an "OK" gesture and a lotus with folding petals are designed and fabricated, which also demonstrate programmable bending actuations and complex shape-deformations. These applications show that the TCP/BOPP actuators have great potential in robotics and biomimetic devices.

2. Materials and methods

2.1. Fabrication of the TCP/BOPP actuator and biomimetic devices

The paper for printing was a commercial product. The thickness was $44\,\mu m$ and the grammage was $18\,g\,m^{-2}$. First of all, a pretreatment step for the paper was needed. The paper was initially placed in a chamber with high humidity (at relative humidity (RH) of 90%) for 5 min to fully absorb water molecules. Then the humid paper was transferred on a hot plate with temperature of $100\,°C$ for $60\,s$, so that the paper desorbed water molecules and returned to the dry state. Then, the pretreated paper was fixed on a piece of copy paper with the aid of tapes. The fabrication of the TCP/BOPP actuator is schematically illustrated in Fig. 1a. First, black toner was directly printed on the pretreated paper by using a commercial laser printer (HP LaserJet Pro CP1025). Second, a commercial BOPP film was attached to the paper tightly with the aid of acrylic ester. Finally, the TCP/BOPP bilayer film was tailored into designed shape to form an actuator. This fast process provides a large-scale, time-saving and mask-free method to fabricate TCP/BOPP

actuator by leveraging the laser printing technology, which reduces the processing time. In the fabrication of biomimetic lotus and rectangular actuators with patterns of gradient grayscale distributions, the BOPP film was attached to the paper surface that is not coated by toner.

2.2. Characterization and measurement

The scanning electron microscope (SEM) images were captured by a field-emission SEM (Hitachi SU8010). The free-end displacements of the actuator were obtained by image postprocessing of optical images and videos, which were captured by a digital camera (SONY ILCE 6000). The calculation method of the bending curvature of actuator is shown in Fig. S1 and Note S1 in Supplemental Information. A NIR light source (Philips BR125) was used for light-driven actuation. The light power density was measured by an infrared power meter (Linshang LS122 A). The temperature was recorded by a laser sight infrared thermometer (Optris LS) with temperature resolution of $0.1\,°C$. The temperature data were obtained from the paper surface of the actuator. An infrared thermal imager (Fluke Ti10) was used to capture the thermal images of the actuator. The weights of samples were measured by a precision balance (YOKEFA1004CS).

3. Results and discussion

3.1. Characterization of TCP/BOPP actuator

As a uniform layer of black toner was printed on the paper, the TCP was black with a thickness of $45\,\mu m$ (Fig. 1b). The cross-sectional SEM image of the printed paper is shown in Fig. S2, which reveals that the toner and paper combined well without any cracks. The photos of two surfaces of the TCP/BOPP actuator are shown in Fig. 1c. As the transparent BOPP film was attached on the toner-coated side of the paper, the BOPP surface of the actuator was black, while the other surface of the paper was white. Fig. 1d demonstrates the layered structure of the TCP/BOPP actuator. The paper and BOPP were well bonded to each other without delamination due to the acrylic ester as adhesive. As shown in a cross-sectional SEM image with higher magnification of the
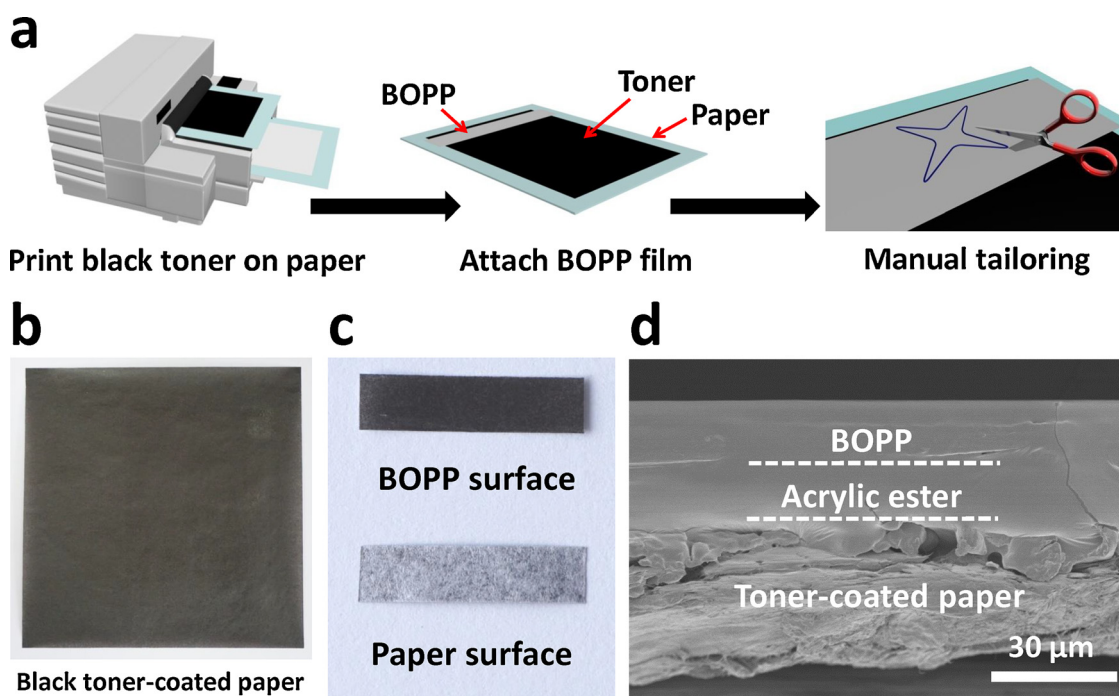

Fig. 1. Fabrication and characterization of the TCP/BOPP actuator. (a) Schematic illustration of the fabrication process of TCP/BOPP actuator. (b) Optical photo of a piece of TCP. (c) Optical photos showing two surfaces of the TCP/BOPP actuator. (d) Cross-sectional SEM image of the TCP/BOPP actuator.

TCP/BOPP actuator (Fig. S3), the toner on paper is tightly combined with acrylic ester.

3.2. NIR light-driven actuation

Photothermal actuators can convert light energy into thermal energy due to the photothermal conversion effect. According to previous studies, the black toner is a complex mixture, generally including carbon black, iron oxide, resin, charge control agents, polymers and inorganic/organic additives [35–37]. The absorption spectrum shows that the TCP can absorb NIR light (Fig. S4). When the TCP is irradiated by NIR light, it can be obviously heated due to the photothermal effect. As shown in Fig. S5, infrared thermal images show that the temperature of TCP/BOPP actuator increased with the increasing of light power. Hence, the TCP is a photothermal conversion material, which can serve as a heating layer to raise the temperature of the TCP/BOPP actuator. In addition, BOPP has a large coefficient of thermal expansion (CTE) of 137 ppm K^{-1}, while the paper has a small CTE of 10 ppm K^{-1} [33]. Therefore, there is a large mismatch in CTEs between paper and BOPP. Moreover, paper is a hydrophilic material, which shrinks when it is heated. Based on these excellent properties of toner, paper and BOPP, they were selected as components of the light-driven actuator based on the photothermal effect.

The bending performance of the TCP/BOPP actuator responding to NIR light was studied at first. A prepared TCP/BOPP actuator (length of 20 mm) was suspended by attaching top of the actuator (5 mm) to a glass slide. The actuator was flat in its initial state (left panel of Fig. 2a). When the actuator was irradiated by the NIR light (550 mW cm^{-2}), it showed a large bending actuation towards paper side (right panel of Fig. 2a). The bending curvature was up to 2.1 cm^{-1}, of which the calculation method is shown in Note S1 and Fig. S1. The light-driven actuation mechanism of the TCP/BOPP actuator is explained as follows. The light energy involved in the NIR light is absorbed by black toner and sequentially converts into thermal energy, which results in the temperature rising of the TCP. The TCP and BOPP are combined tightly, so the temperature of the TCP/BOPP actuator also increased. As the CTE of BOPP is much larger than that of paper, the thermal expansion of BOPP will be larger than that of paper with the same temperature rising. Meanwhile, the temperature rising will also cause the shrinking of paper as the paper desorbs water molecules to ambient environment, which further increases the volume change difference between BOPP and paper. Then, thermal stress of the TCP/BOPP bilayer film, which is generated by the interfacial mismatch between TCP and BOPP, also increases with temperature rising. The maximum thermal stress is calculated to be 19.4 MPa when the actuator is irradiated by NIR light (550 mW cm^{-2}) for 10 s (Note S2). In a word, the dual-mode actuation mechanism results in the bending actuation of the actuator towards paper side.

The temperature and bending curvature of the TCP/BOPP actuator with different light power are shown in Fig. 2b. When the actuator was irradiated by low light power (50 mW cm^{-2}) for 10 s, the temperature was only 26.0 °C and the bending curvature was as small as 0.1 cm^{-1}. When the actuator was irradiated by high light power (550 mW cm^{-2}), the temperature was as high as 70.4 °C and the curvature was up to 2.1 cm^{-1}. Hence, Fig. 2b also shows the controllability of the TCP/BOPP actuator. It is obvious that when the light power is increased, more light energy is converted into thermal energy by black toner, which directly results in higher temperature of the TCP/BOPP actuator. Therefore, the bending curvature of the actuator gets larger with higher light power.

The temperature and curvature variation trend were studied as well. When the TCP/BOPP actuator was irradiated by NIR light for 10 s, the temperature and curvature of the actuator increased synchronously, as shown in Fig. 2c. However, when the NIR light was turned off, the variation of temperature and curvature were different. The temperature decreased quickly to 26 °C in 15 s, while the actuator returned back to the initial state in 170 s. Therefore, the temperature decreased much

faster than the curvature. The asynchronism of temperature and curvature can be attributed to the hygroexpansion effect of the paper. With NIR light irradiation, the paper desorbed water molecules within it. After NIR light was turned off, the paper needs more time to reach a new balance in moisture contents between the paper and the ambient. Hence, although the temperature almost returned to initial temperature, the paper still absorbed water molecules from surroundings, resulting in the much slower curvature recovery of the TCP/BOPP actuator. Such phenomenon also proves that the actuation is based on the dual-mode actuation mechanism.

Moreover, the repeatability of the bending performance of the actuator was tested. The light power density in the repeatability test was 300 mW cm^{-2}. As shown in Fig. S6, the bending curvature had no degradation after 100 cycles, which indicates outstanding stability and reliability of the light-driven actuation of TCP/BOPP actuator. The cross-sectional SEM image of the TCP/BOPP actuator after repeatability test is shown in Fig. S7. It shows that the TCP and BOPP film were still combined tightly without delamination.

3.3. Shape-deformation of actuators with different grayscale patterns

In particular, the TCP/BOPP actuator is able to have different grayscale patterns by changing the amount of black toner printed on paper, which is based on the unique laser printing technology. Fig. 2d shows the TCP films with 100% black, 50% black and 15% black, respectively. The different grayscale patterns were obtained by tuning the color in PowerPoint of Microsoft Office. The 100% black was pure black. The 50% black was 50% deeper than pure white. The 15% black was 15% deeper than pure white. The TCP with deeper black color shows higher absorption ability in wavelength from visible to NIR light, as shown in Fig. S8. Fig. 2e shows the temperature of TCP/BOPP actuators with different grayscale patterns (100% black, 50% black and 15% black), when they were irradiated by different NIR light power. With NIR light irradiation (550 mW cm^{-2}) for 10 s, the temperature of actuators with different grayscale patterns (100% black, 50% black and 15% black) were measured to be 70.4 °C, 62.0 °C, 44.6 °C, respectively. The corresponding curvatures of the TCP/BOPP actuators with different grayscale patterns (100% black, 50% black and 15% black) are shown in Fig. S9. Hence, the TCP with deeper black color can absorb and convert more light energy into thermal energy, leading to higher temperature and larger bending actuation of the TCP/BOPP actuator.

It is worth mentioning that because the laser printing technology is capable of controlling the grayscale, and thus the light absorption ability of the TCP, programmable shape-deformation of the TCP/BOPP actuator can be conveniently achieved by tuning bending rates and amplitudes of the actuators. As shown in Fig. 2f, the TCP/BOPP actuator with deeper black color shows large bending amplitudes when irradiated by the same NIR light power (550 mW cm^{-2}). The bending curvature of the TCP/BOPP actuator with 100% black was 2.1 cm^{-1} after irradiated by NIR light for 10 s, while the actuator with 15% black showed a much smaller curvature of 0.8 cm^{-1}. The average bending rate of the TCP/BOPP actuator with 100% black was 0.21 cm^{-1} s^{-1}, which was 2.6 times faster than that of the actuator with 15% black. Hence, the bending amplitudes and rates of the TCP/BOPP actuators can be precisely controlled by printing actuators with different grayscale patterns, demonstrating programmable shape-deformations, which are owing to the advantage of laser printing technology.

3.4. Shape-deformation of actuators with gradient grayscale patterns

To realize programmable complex shape-deformations, it is necessary to locally and distinctively control the deformation of specific parts of the actuators. With the help of laser printing technology, patterns with gradient grayscale distribution can be easily obtained by using the "gradient fill" option in the PowerPoint of Microsoft Office. In this way, different parts of the actuators have different black color, so that each
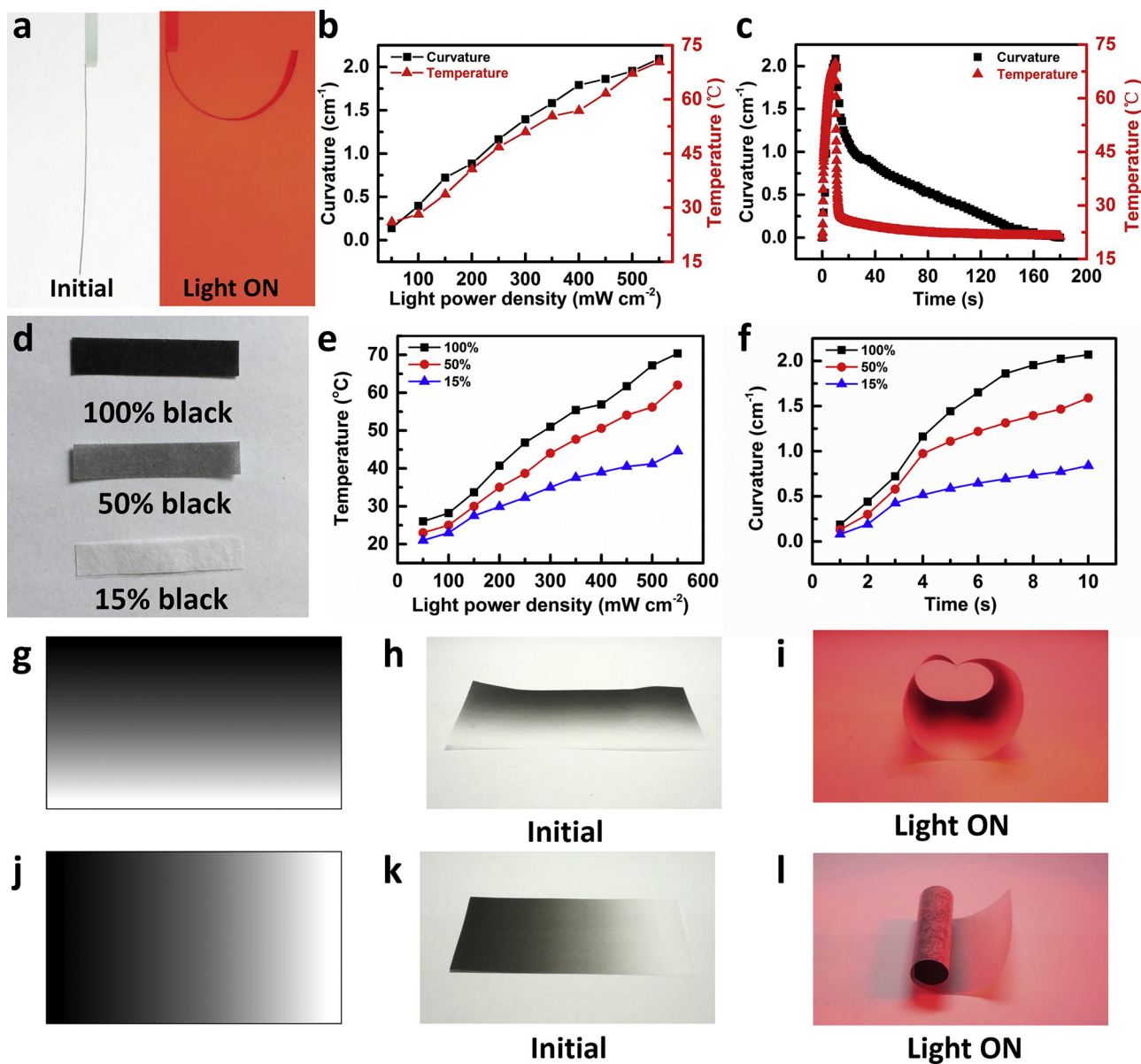
Fig. 2. TCP/BOPP actuator responding to NIR light. (a) Optical photos of the initial state of TCP/BOPP actuator (left panel) and the of the actuator irradiated by NIR light (550 mW cm^{-2}) for 10 s (right panel). (b) Curvature and temperature of the TCP/BOPP actuator as a function of light power density. (c) Curvature and temperature of the TCP/BOPP actuator as a function of time. (d) Optical photos of TCP films with different grayscale patterns (100% black, 50% black and 15% black). (e) Temperature of the TCP/BOPP actuators with different grayscale patterns as a function of light power density. (f) Curvature of the TCP/BOPP actuators with different grayscale patterns as a function of time (light power density of 550 mW cm^{-2}). The dimensions of the TCP/BOPP actuators were 20 mm × 2 mm × 75 μm (length × width × thickness). (g) Rectangular pattern with a gradient grayscale distribution (along the short side). (h) Optical photo showing the initial state of the TCP/BOPP actuator with the pattern corresponding to (g). (i) Optical photo showing the TCP/BOPP actuator with the pattern corresponding to (g) deforms into a complex 3D shape (anomalous tube), when driven by NIR light. (j) Rectangular pattern with a gradient grayscale distribution (along the long side). (k) Optical photo showing the initial state of the TCP/BOPP actuator with the pattern corresponding to (j). (l) Optical photo showing the TCP/BOPP actuator with the pattern corresponding to (j) deforms into another complex 3D shape (helical cylinder), when driven by NIR light.

part of actuators deforms diversely, resulting in programmable complex shape-deformations. Fig. 2g shows a rectangular pattern (80 mm × 40 mm, length × width) with a gradient grayscale distribution along the short side, which is designed by computer. Then, this pattern was printed on the paper and a rectangular TCP/BOPP actuator was fabricated. The initial state of the actuator was flat (Fig. 2h). After irradiated by the NIR light (300 mW cm^{-2}), the actuator deformed into a complex 3D shape, which looked like an anomalous tube with one large opening at one end (Fig. 2i, Movie S1). On the other hand, Fig. 2j shows another rectangular pattern with the same dimension. However, the gradient grayscale distribution is along the long side. Fig. 2k shows that the initial state of the TCP/BOPP actuator with this pattern was also flat.

After irradiated by the NIR light (300 mW cm^{-2}), the actuator deformed into another complex 3D shape (a helical cylinder). As shown in Fig. 2l and Movie S2, one end of the actuator showed an ultralarge curling deformation (bending angle > 360°), while the other end of the actuator showed only a slight bending deformation. The reason for obtaining such complex 3D shapes is that the TCP with deeper black color can absorb and convert more light energy into thermal energy, leading to higher temperature of the corresponding part of the TCP/BOPP actuator. The temperature distributions of the TCP/BOPP actuators performing programmable complex 3D shapes are shown in Fig. S10. Hence, the TCP/BOPP actuator with the patterns of gradient grayscale distribution will have different amplitudes of bending
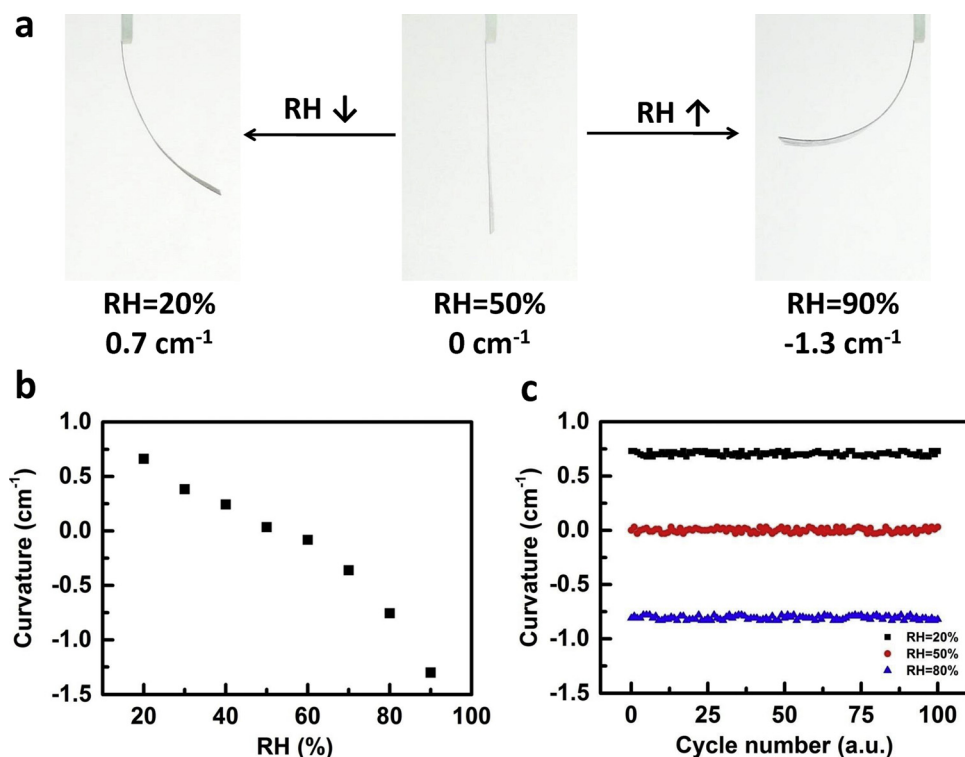
Fig. 3. TCP/BOPP actuator responding to humidity. (a) Optical photos of the TCP/BOPP actuator at RH of 20% (left panel), RH of 50% (middle panel) and RH of 90% (right panel). (b) Curvature of the TCP/BOPP actuator as a function of RH. (c) Repeatability test of the TCP/BOPP actuator undergoing repeated RH changes between 20% and 80%. The dimensions of the TCP/BOPP actuators were 20 mm × 2 mm × 75 μm (length × width × thickness).

actuation in different parts of the actuator, leading to the programmable complex shape-deformations. In a word, programmable complex 3D shape-deformations can be achieved based on the platform of TCP/BOPP actuators fabricated by laser printing technology.

3.5. Humidity-driven actuation

Due to the hygroexpansion effect of paper, the TCP is highly sensitive to humidity changes. Hence, the TCP/BOPP actuator is expected to be driven by humidity as well. A TCP/BOPP actuator with 100% black color was fabricated at RH of 50%. The middle panel of Fig. 3a shows that the actuator (20 mm long) was suspended with a flat state. Top end of the actuator (5 mm) was fixed to a glass slide. When the RH increased to 90%, the actuator showed a large bending actuation to the BOPP side in 60 s. The bending curvature was as large as 1.3 cm^{-1} (right panel of Fig. 3a). On the contrary, when the RH decreased to 20%, the actuator showed a bending actuation towards the paper side in 60 s. The curvature was 0.7 cm^{-1} (left panel of Fig. 3a). The influence of the humidity on the bending curvature was also studied. The humidity-driven actuation is attributed to the hygroexpansion effect of paper. When the RH increases (from 50% to 90%), the paper adsorbs water molecules and expands, while the BOPP is hydrophobic and is inert to humidity without volume changes. As the TCP and BOPP layers are tightly combined, different volume change between them will result in the TCP/BOPP actuator bending towards the BOPP side. Conversely, RH decrease (from 50% to 20%) causes the shrinking of paper, while the volume of BOPP film remains the same. Hence, the TCP/BOPP actuator bends to the paper side. We define the curvature bending towards the paper side as a positive value and define that bending towards the BOPP side as a negative value. As presented in Fig. 3b, when the RH increased from 20% to 90%, the curvature of the TCP/BOPP actuator changed from 0.7 to -1.3 cm^{-1}. Finally, a repeatability test result of the TCP/BOPP actuator when driven by humidity is shown in Fig. 3c. The TCP/BOPP actuator was under a repeated humidity alteration between 20% and 80% for 100 cycles. The humidity-driven actuation performance of the actuator remained stable after the repeatability test.

3.6. Biomimetic applications

Intelligence, sophistication and versatility of nature biology are continuous sources of inspiration for biomimetic systems. Mimicking the natural biology intelligence system to fabricate biomimetic systems are still great challenges in the field of actuators. To extend the utilizations of TCP/BOPP actuator, three biomimetic applications are fabricated to show the capability of tunable and varied shape-deformations.

An iris in the eye has an ability to change its pupil size, so as to adjust different light transmission into the eye. Firstly, we fabricated an iris-like actuator that can perform automatic closing-opening in response to the incident light. A closing iris-shaped pattern was designed by computer, as shown in Fig. 4a. The fabricated biomimetic iris is shown in Fig. 4b, which was initially fabricated at low RH of 35%. Therefore, when the biomimetic iris was placed at room RH of 50%, it automatically opened up (Fig. 4c). When irradiated by NIR light (300 mW cm^{-2}) for 10 s, the biomimetic iris bent inward and the pupil closed (Fig. 4d, Movie S3). After turning off the NIR light, the biomimetic iris automatically returned to the initial opening state. Hence, the biomimetic iris closes under high light intensity and reaches a small pupil size, while it opens under low light intensity, mimicking the self-adjustment nature iris.

Secondly, a biomimetic hand was fabricated. An integrated hand-shaped pattern was designed by computer, in which different grayscale and gradient grayscale distribution were both well demonstrated in one device (Fig. 4e). The biomimetic hand included 5 fingers, having different grayscales. The thumb and index finger were 100% black. The middle finger was 50% black. The ring finger was 15% black and the little finger was 0% black (100% white). The palm was a rectangle with a gradient grayscale distribution (grayscale decreased from left to right). The hand-shaped pattern was then printed on paper and the biomimetic hand-shape actuator was fabricated (Fig. 4f). The biomimetic hand was initially clamped by two vertical glass slides (Fig. 4g). When the NIR light was turned on (300 mW cm^{-2}), the fingers were bending with different bending rates. The thumb and index finger had the deepest black color (100% black), showing the fastest bending rates.
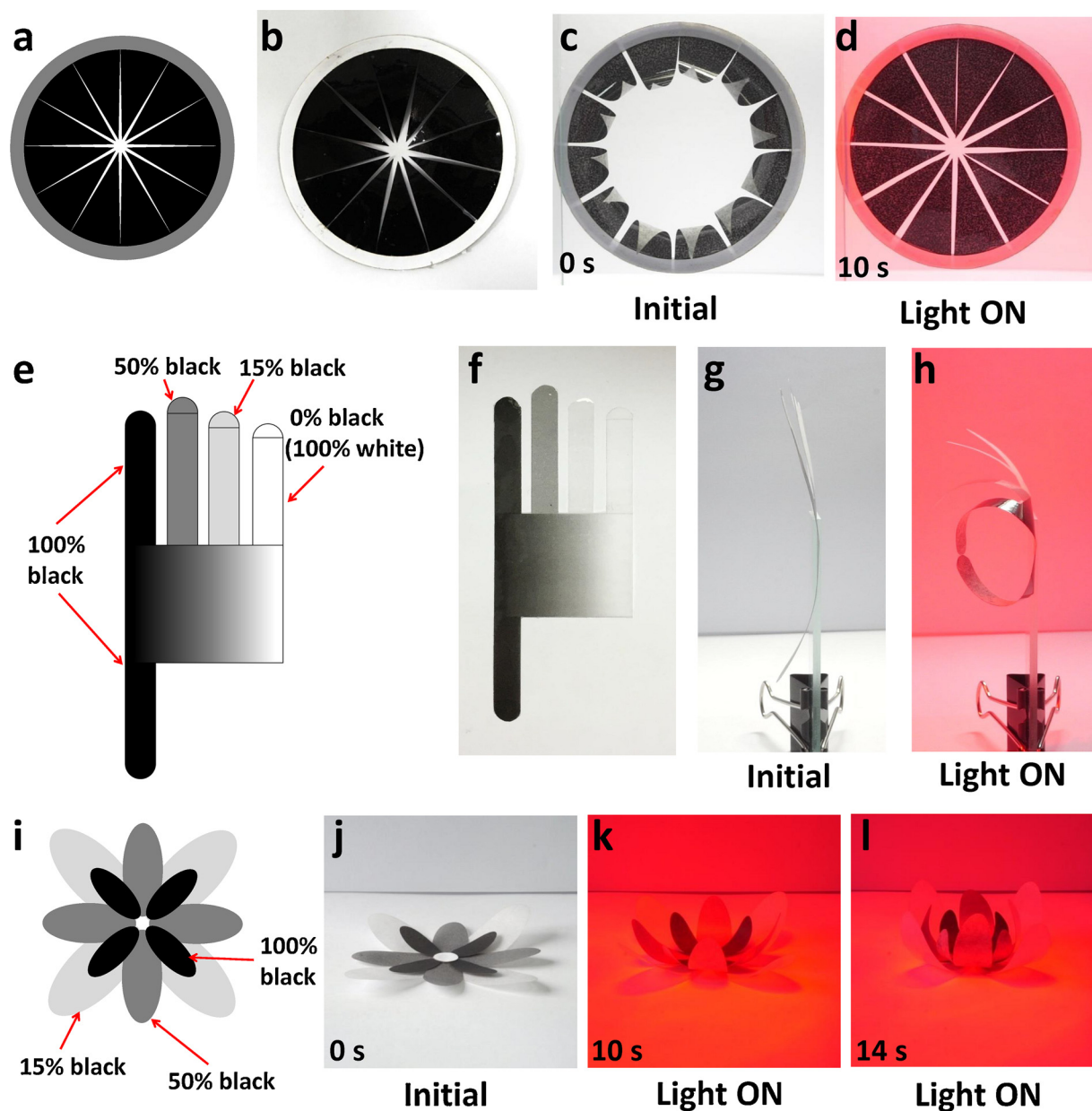
Fig. 4. Biomimetic applications. (a) Pattern of the biomimetic iris designed by computer. (b) Optical photo showing the fabricated biomimetic iris at low RH of 35%. (c) Optical photo showing the initial opening state of the biomimetic iris at room RH of 50%. (d) Optical photo showing the closing state of the biomimetic iris when irradiated by NIR light (300 mW cm^{-2}). (e) Pattern of the biomimetic hand designed by computer. (f) Optical photo showing the fabricated biomimetic hand-shape actuator. (g) Optical photo showing the initial state of the biomimetic hand. (h) Optical photo showing that the biomimetic hand performs a programmable complex 3D shape ("OK" gesture) when irradiated by NIR light (300 mW cm^{-2}). (i) Pattern of the biomimetic lotus designed by computer. (j) Optical photo of the fabricated biomimetic lotus. (k–l) Optical photos showing the folding process of the biomimetic lotus when driven by NIR light (500 mW cm^{-2}).

The bending rates of the other three fingers were decreasing in sequence. After NIR light irradiation for 10 s, the finger tips of the thumb and the index finger could touch to each other, while the other three fingers demonstrated different bending amplitudes. Interestingly, the biomimetic hand finally demonstrated a complex 3D shape, which looked like an "OK" gesture (Fig. 4h, Movie S4).

At last, as the TCP/BOPP actuators can have different grayscale patterns by leveraging the laser printing technology, a biomimetic lotus was designed and fabricated. A blooming lotus-shaped pattern was designed by computer, as shown in Fig. 4i. The biomimetic lotus had 12 petals, forming three layers. The grayscale decreased gradually from inside layer to outside layer (inside 100% black, middle 50% black, and outside 15% black). The fabricated biomimetic lotus was shown in Fig. 4j. When the biomimetic lotus was irradiated by NIR light (500 mW cm^{-2}), three-layer petals folded with different bending rates, as shown in Fig. 4k-l and Movie S5. The petals of inside layer had the deepest black color (100% black), so they absorbed more light energy than the other petals and demonstrated the fastest bending rate. The bending rate of the middle petals showed a slower bending rate, while the outside petals had the slowest bending rate.

4. Conclusions

In summary, we propose a laser printing technology to fabricate dual-responsive TCP/BOPP actuators with programmable complex shape-deformations. More importantly, the bending rates and amplitudes of the actuators can be precisely programmed and controlled by changing the grayscale of patterns with computer assistance. The TCP/

BOPP actuator shows a large bending curvature ($2.1\,cm^{-1}$) with NIR light irradiation due to the dual-mode actuation mechanism. One mechanism is thermal expansion mismatch between the paper and BOPP. The other mechanism is the hygroexpansion effect of paper. The actuator also shows a bending curvature of $1.3\,cm^{-1}$ when driven by humidity. Finally, a series of biomimetic devices are displayed, which further demonstrate programmable complex shape-deformations based on the TCP/BOPP actuators. With further improvement, the TCP/BOPP actuators will not only realize programmable complex shape-deformation on the basis of the facile printing strategy, but also be useful in the field of lab-on-paper devices, artificial muscles, robotics and versatile biomimetic applications.

Declarations of interests

Acknowledgements

Appendix A. Supplementary data

Supplementary material related to this article can be found, in the online version, at doi:https://doi.org/10.1016/j.snb.2018.11.067.

References

[1] Y. Liu, B. Shaw, M.D. Dickey, J. Genzer, Sequential self-folding of polymer sheets, Sci. Adv. 3 (2017) e1602417.
[2] Y. Zhang, M. Tan, Programmable light-activated gradient materials based on graphene-polymer composites, Adv. Mater. Interfaces 5 (2018) 1701374.
[3] H. Lim, T. Park, J. Na, C. Park, B. Kim, E. Kim, Construction of a photothermal venus flytrap from conductive polymer bimorphs, NPG Asia Mater. 9 (2017) e399.
[4] J. Deng, J. Li, P. Chen, X. Fang, X. Sun, Y. Jiang, W. Weng, B. Wang, H. Peng, Tunable photothermal actuators based on a pre-programmed aligned nanostructure, J. Am. Chem. Soc. 138 (2016) 225–230.
[5] Y. Hu, G. Wu, T. Lan, J. Zhao, Y. Liu, W. Chen, A graphene-based bimorph structure for design of high performance photoactuators, Adv. Mater 27 (2015) 7867–7873.
[6] X. Zhang, Z. Yu, C. Wang, D. Zarrouk, J. Seo, J. Cheng, A. Buchan, K. Takei, Y. Zhao, J. Ager, J. Zhang, M. Hettick, M. Hersam, A. Pisano, R. Fearing, A. Javey, Photoactuators and motors based on carbon nanotubes with selective chirality distributions, Nat. Commun. 5 (2014) 2983.
[7] S. Yao, J. Cui, Z. Cui, Y. Zhu, Soft electrothermal actuators using silver nanowire heaters, Nanoscale 9 (2017) 3797–3805.
[8] L. Chen, M. Weng, Z. Zhou, Y. Zhou, L. Zhang, J. Li, Z. Huang, W. Zhang, C. Liu, S. Fan, Large deformation curling actuators based on carbon nanotube composite advanced structure design and biomimetic application, ACS Nano 9 (2015) 12189–12196.
[9] L.Z. Chen, C.H. Liu, C.H. Hu, S.S. Fan, Electrothermal actuation based on carbon nanotube network in silicone elastomer, Appl. Phys. Lett. 75 (2008) 263104.
[10] Z. Wang, F. Wang, Y. Zhao, Tap dance of a water droplet, P. Roy. Soc. A-Math. Phy. 468 (2012) 2485–2495.
[11] Y. Zhang, H. Jiang, F. Li, Y. Xia, Y. Lei, X. Jin, G. Zhang, H. Li, Graphene oxide based moisture-responsive biomimetic film actuators with nacre-like layered structures, J. Mater. Chem. A 5 (2017) 14604–14610.
[12] D. Han, Y. Zhang, H. Jiang, H. Xia, J. Feng, Q. Chen, H. Xu, H. Sun, Moisture-responsive graphene paper prepared by self-controlled photoreduction, Adv. Mater. 27 (2015) 332–338.
[13] D. Han, Y. Zhang, Y. Liu, Y. Liu, H. Jiang, B. Han, X. Fu, H. Ding, H. Xu, H. Sun, Bioinspired graphene actuators prepared by unilateral UV irradiation of graphene oxide papers, Adv. Funct. Mater. 25 (2015) 4548–4557.
[14] M. Wang, X. Tian, R. Ras, O. Ikkala, Sensitive humidity-driven reversible and bidirectional bending of nanocellulose thin films as bio-inspired actuation, Adv. Mater. Interfaces 2 (2015) 1500080.
[15] H. Cheng, J. Liu, Y. Zhao, C. Hu, Z. Zhang, N. Chen, L. Jiang, L. Qu, Graphene fibers with predetermined deformation as moisture-triggered actuators and robots, Angew. Chem. Int. Ed. 52 (2013) 10482–10486.

[16] Y. Kim, M. Liu, Y. Ishida, Y. Ebina, M. Osada, T. Sasaki, T. Hikima, M. Takata, T. Aida, Thermoresponsive actuation enabled by permittivity switching in an electrostatically anisotropic hydrogel, Nat. Mater. 14 (2015) 1002–1007.
[17] S. Jiang, F. Liu, A. Lerch, L. Ionov, S. Agarwal, Unusual and superfast temperature-triggered actuators, Adv. Mater. 27 (2015) 4865–4870.
[18] Y. Jin, B. Shin-Il Kim, W. Lee, C. Lee, H. Kim, K. Song, S. Jang, G. Kwak, Phase-change hybrids for thermo-responsive sensors and actuators, NPG Asia Mater. 6 (2014) e137.
[19] J. Kim, S. Chung, S. Choi, H. Lee, J. Kim, S. Kwon, Programming magnetic anisotropy in polymeric microactuators, Nat. Mater. 10 (2011) 747–752.
[20] H. Lin, J. Gong, M. Eder, R. Schuetz, H. Peng, J. Dunlop, J. Yuan, Programmable actuation of porous poly(ionic liquid) membranes by aligned carbon nanotubes, Adv. Mater. Interfaces 4 (2017) 1600768.
[21] H. Lin, J. Gong, H. Miao, R. Guterman, H. Song, Q. Zhao, J. Dunlop, J. Yuan, Flexible and actuating nanoporous poly(ionic liquid) paper-based hybrid membranes, ACS Appl. Mater. Interfaces 9 (2017) 15148–15155.
[22] H. Chen, Y. Li, Y. Liu, T. Gong, L. Wang, S. Zhou, Highly pH-sensitive polyurethane exhibiting shape memory and drug release, Polym. Chem. 5 (2014) 5168–5173.
[23] H. Zeng, O. Wani, P. Wasylczyk, R. Kaczmarek, A. Priimagi, Self-regulating iris based on light-actuated liquid crystal elastomer, Adv. Mater. 29 (2017) 1701814.
[24] M. Hamedi, V. Campbell, P. Rothemund, F. Güder, D. Christodouleas, J. Bloch, G. Whitesides, Electrically activated paper actuators, Adv. Funct. Mater. 26 (2016) 2446–2453.
[25] L. Hines, K. Petersen, G.Z. Lum, M. Sitti, Soft actuators for small-scale robotics, Adv. Mater. 29 (2017) 1603483.
[26] L. Chen, C. Liu, K. Liu, C. Meng, C. Hu, J. Wang, S. Fan, High performance, low voltage, and easy operable bending actuator based on aligned carbon nanotube/polymer composites, ACS Nano 5 (2011) 1588–1593.
[27] Z. Zeng, H. Jin, L. Zhang, H. Zhang, Z. Chen, F. Gao, Z. Zhang, Low-voltage and high-performance electrothermal actuator based on multi-walled carbon nanotube/polymer composites, Carbon 84 (2015) 327–334.
[28] Y. Hu, T. Lan, G. Wu, Z. Zhu, W. Chen, A spongy graphene based bimorph actuator with ultra-large displacement towards biomimetic application, Nanoscale 6 (2014) 12703–12709.
[29] A. Nojoomi, H. Arslan, K. Lee, K. Yum, Bioinspired 3D structures with programmable morphologies and motions, Nat. Commun. 9 (2018) 3705.
[30] X. Peng, T. Liu, Q. Zhang, C. Shang, Q. Bai, H. Wang, Surface patterning of hydrogels for programmable and complex shape deformations by ion inkjet printing, Adv. Funct. Mater. 27 (2017) 1701962.
[31] H. Yang, W. Leow, T. Wang, J. Wang, J. Yu, K. He, D. Qi, C. Wan, X. Chen, 3D printed photoresponsive devices based on shape memory composites, Adv. Mater. 29 (2017) 1701627.
[32] L. Chen, M. Weng, P. Zhou, L. Zhang, Z. Huang, W. Zhang, Multi-responsive actuators based on a graphene oxide composite: intelligent robot and bioinspired applications, Nanoscale 9 (2017) 9825–9833.
[33] M. Weng, P. Zhou, L. Chen, L. Zhang, W. Zhang, Z. Huang, C. Liu, S. Fan, Multiresponsive bidirectional bending actuators fabricated by a pencil-on-paper method, Adv. Funct. Mater. 26 (2016) 7244–7253.
[34] M. Amjadi, M. Sitti, High-performance multiresponsive paper actuators, ACS Nano 10 (2016) 10202–10210.
[35] N. Verma, R. Kumar, V. Sharma, Analysis of laser printer and photocopier toners by spectral properties and chemometrics, Spectrochim. Acta A. 196 (2018) 40–48.
[36] M. Ataeefard, Production of black toner through emulsion aggregation of magnetite, carbon black, and styrene-acrylic co-polymer: investigation on the effect of variation in components, J. Compos. Mater. 49 (2014) 1553–1561.
[37] M. Szynkowska, K. Czerski, T. Paryjczak, A. Parczewski, Ablative analysis of black and colored toners using LA-ICP-TOF-MS for the forensic discrimination of photocopy and printer toners, Surf. Interface Anal. 42 (2010) 429–437.

Dr. Luzhuo Chen received his B. Sc. from Xiamen University, China (2006). Then, he was recommended to join Prof. Shoushan Fan's group as a Ph. D. candidate at Tsinghua University, China and received his Ph. D. in 2011. He is currently an associate professor in Fujian Normal University, China. His research interests include smart actuators, sensors, intelligent robots, chromic materials and energy conversion & storage devices.

Mr. Mingcen Weng received his Bachelor's degree in 2014 from Fujian Normal University. He is currently a Ph. D. candidate in Dr. Luzhuo Chen's group in College of Physics and Energy of Fujian Normal University. His research interests focus on carbon-based actuators.

Dr. Feng Huang has obtained his Ph. D. degree in University of Science and Technology of China in 2009. He is currently an associate professor in Fujian Normal University. His current research includes energy conversion materials as well as the localized surface plasmon resonance in nanocrystals and nano-heterostructures.

Dr. Wei Zhang received her B. Sc. from Northeast Normal University, China (2006). She received her Ph. D. from Institute of Physics, Chinese Academic of Sciences, China (2011). She worked on the new technology of polymer at Global Innovation Center (Beijing) of Proctor and Gamble (P&G) Company (2011–2014). Now she is an associate professor in Fujian Normal University. Her research interests involve actuator material design and unique properties of 2D materials.